Microstructure and Residual Stresses in Dissimilar Mg–Al–Zn–Alloy Single Overlap Laser Beam Welds

Article *in* Materials Science Forum · January 2008

DOI: 10.4028/www.scientific.net/MSF.571-572.361

6 authors, including:

Rodrigo Santiago Coelho
SENAI CIMATEC Bahia
41 PUBLICATIONS **616** CITATIONS
SEE PROFILE

Aleksander Kostka
Ruhr-Universität Bochum
166 PUBLICATIONS **4,067** CITATIONS
SEE PROFILE

Haroldo Cavalcanti Pinto
University of São Paulo
133 PUBLICATIONS **725** CITATIONS
SEE PROFILE

Stefan Riekehr
Helmholtz-Zentrum Geesthacht
88 PUBLICATIONS **872** CITATIONS
SEE PROFILE

Materials Science Forum Vols. 571-572 (2008) pp 361-366
online at http://www.scientific.net

Online available since 2008/Mar/07

Microstructure and Residual Stresses in Dissimilar Mg-Al-Zn-alloy Single Overlap Laser Beam Welds

R.S. Coelho[1], A. Kostka[1,*], H. Pinto[1], S. Riekehr[2], M. Koçak[2], A.R. Pyzalla[1]

[1] Max-Planck-Institut für Eisenforschung GmbH, 40237 Düsseldorf, Germany
[2] GKSS Research Centre GmbH, 21502 Geesthacht, Germany

*Corresponding author: Tel.: +49 (0)211 6792989, E-mail address: a.kostka@mpie.de

Keywords*:* Mg; microstructure; residual stress; laser welding; mechanical properties

Abstract

Microstructure, hardness and residual stresses of the laser beam overlap welds between AZ31B sheets and AZ31, AZ61 and AZ80 extruded profiles are investigated using microscopy and X-ray diffraction. The result of the investigations reveal that weld microstructure, the size of the HAZ, precipitate density and the maximum compressive residual stress values depend strongly on the Al content of the weld zone of two Mg-alloys.

Introduction

Reduction of weight of transport systems has strong economic and ecologic impacts and this can be achieved by either using higher strength materials or material-mix design. Mg- and its alloys, being the lightest available structural metallic material, are increasingly applied in replacement of Al-alloys in specific structural applications [1-3] using single or dissimilar joint configurations. Currently, wrought rolled sheets and extruded profiles of Mg-Al-Zn Mg-alloys are commercially used [4,5]. Extruded Mg-alloys formerly often failed to satisfy the stringent requirements of automotive and aircraft industries on mechanical properties. Recent progress in extrusion of Mg-alloys showed that by choosing appropriate extrusion processes and alloying constituents, for instance the Al content, significant improvements can be made [6]. As the most favourable alloying constituent, Al improves the strength and hardness of the Mg-alloy, e.g. AZ80 (8 wt.-% Al) has a higher yield and ultimate strengths under both compression and tension loadings compared to AZ31. Increasing the Al content further results in an increase of ($Mg_{17}(Al,Zn)_{12}$) precipitation in a network along the grain boundaries, which obstructs grain growth in the extruded products, but, decreases elongation to fracture [1,6,7].

In order to further widen the field of Mg-alloy application, suitable joining processes are needed particularly in dissimilar configurations. Tungsten inert gas welding (TIG), laser beam welding (LBW), friction stir welding (FSW) and electron beam welding (EBW) have been applied for welding Mg-alloys in similar and dissimilar configurations [4,8-11]. In case of dissimilar joints, the differences in the physical and mechanical properties of the constituents result in gradients in composition and microstructure as well as strongly inhomogeneous internal stress states. Nd:YAG laser beam welding is particularly attractive for welding dissimilar Mg-alloys because of its smaller wave length than CO_2 lasers as well as high precision and process speed, low heat input and consequently narrow heat affected zone (HAZ) and low distortion of the welds [4].

Here, Nd:YAG laser beam welding was applied for joining AZ31B rolled sheets to AZ31, AZ61 and AZ80 extruded L-shape profiles in single overlap configuration. The aim of this study is to investigate the evolved microstructures and residual stresses of dissimilar Mg-alloy weld joints both in terms of sheet and profile materials as well as variation of Al-content.

Experimental Details

Materials. Wrought rolled sheets of AZ31B Mg-alloy were purchased at Sinomag, China. Wrought extruded L-shape profiles of AZ31, AZ61 and AZ80 were produced at the Extrusion Research and Development Centre of TU Berlin, Germany. The chemical compositions of the four Mg-alloys used in this study are shown in Table 1.

Table 1. Chemical composition of the wrought Mg-Al-Zn Mg-alloys in wt.% .

Alloy	Al	Zn	Mn	Ca	Si	Cu	Ni	Fe
AZ31B **rolled**	3.3-3.6	0.45-0.53	0.27-0.29	-	<0.10	<0.05	<0.005	<0.02
AZ31 **extruded**	2.5-3.5	0.6-1.4	0.20 min	0.40	0.10	0.05	0.005	0.005
AZ61 **extruded**	5.8-7.2	0.4-1.5	0.15 min	-	0.10	0.05	0.005	0.005
AZ80 **extruded**	7.0-8.1	0.4-1.0	0.30 min	-	0.30	0.10	0.01	-

Welding Procedure. Nd:YAG LBW was used to join the Mg-Al-Zn Mg-alloys at GKSS Research Centre, Geesthacht, Germany. Single overlap welds were manufactured by joining AZ31B rolled sheets of $150\times200\times2mm^3$ sizes to AZ31, AZ61 and AZ80 extruded L-shape profiles (Fig. 1). The welding parameters chosen were: 2.2kW laser power, 4m/min welding speed, -2mm focal point and 16 l/min helium shielding gas at the top side. The welds were produced without wire and no post-welding heat treatment was performed.

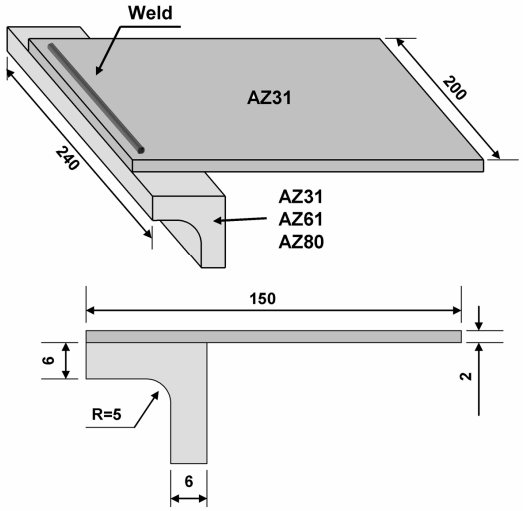

Fig. 1. Schematic overview of Mg-Al-Zn Mg-alloys joined by Nd:YAG LBW, single overlap configuration without wire.

Microscop. Microstructure analysis was carried out by optical microscopy (OM) and scanning electron microscopy (SEM) with an electron back scattering diffraction system (EBSD). The specimens were sectioned, ground, polished using lubricant without water and etched. The EBSD measurements in the fusion zone and the base material covered sample areas of $1500\times1500\mu m^2$ and inverse pole figures were generated from each grain map determined.

Mechanical properties. Microhardness measurements were performed on the weld cross section according to ASTM E384-99 standard. The analyses were performed both in the rolled sheet (Line 2) and the extruded profile (Line 3), as shown in Fig. 2

Residual stress analysis. Residual stress (RS) analysis was carried out using an X-ray tube at MPIE and by employing synchrotron X-ray diffraction at the experimental station G3 at DORIS III at HASYLAB at DESY, Hamburg, using the $\sin^2\psi$ technique [12]. The radiation energy used was 6.9keV and the beam size was set to $1.5\times1.5mm^2$. The measurements were carried out for a $\sin^2\psi$-range of 0 to 0.8, with a step size of 0.2, using the Mg (112) reflection. Residual stresses in both the longitudinal (welding) and transversal directions were determined on top of the overlap joints as shown in Fig. 2, Line 1 (-6 to +30mm distance from the weld centreline). In order to compare the in-depth RS distribution in similar and dissimilar joints, further measurements were performed in the transversal and normal directions of electro-chemically etched cross sections (Fig.2, Lines 2 and 3).

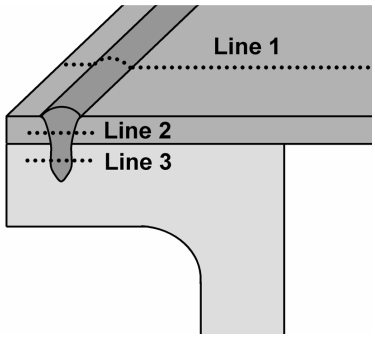

Fig. 2. Scheme of performed RS analyses.

Results and discussions

Weld microstructure. OM analysis reveals that applying the same welding parameters, the width and the depth of the fusion zone increase from AZ31 to AZ61 to AZ81. Increasing the Al-content (by using of different extruded L-shape profiles) decreases the solidus temperature and thermal conductivity of the Mg-alloy [15,16]. OM analysis also shows small pore formation at the interface between the dissimilar welded materials (marked by an arrow, Fig. 3) due to the presence of gap and inaccessibility of these regions by the Helium shielding gas, resulting in oxidation of the molten Mg-alloy.

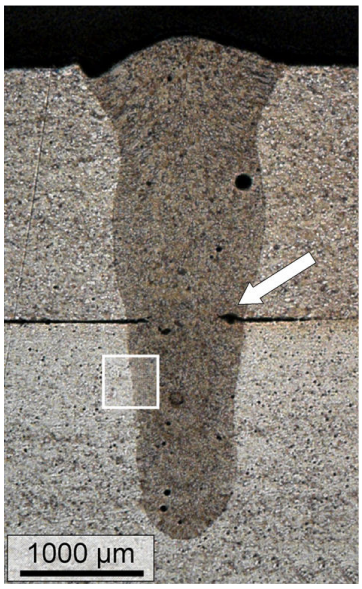

Fig. 3. OM analyses of the cross section of an AZ31B-AZ31 weld.

Further investigation applying SEM-EBSD analysis of the cross section (area marked in Fig. 3) reveals the influence of the Al-content on the microstructural evolution of the fusion zones of the profile material parts (Fig. 4). SEM analysis shows a large heat affected zone (HAZ) increasing the Al-content, which is characterized by the presence of precipitates ($Mg_{17}(Al, Zn)_{12}$) along the grains boundaries (Fig. 4) [9,13,14]. The amount of precipitates in the HAZ and in the fusion zone increases with increase Al-content. The high affinity of these precipitates with oxygen may result in some MgO, Al_2O_3 or $MgAl_2O_4$ formation [13,14]. In the AZ31B-AZ80 combination, partial melting presumably proceeds from the fusion zone in outward direction along the $Mg_{17}(Al,Zn)_{12}$ particles (low melting point, Tm~460°C) that were mainly aligned along the grain boundaries of the base material [9].

EBSD analysis show that in case of the AZ31B-AZ80 weld an about 100µm wide layer with small equiaxed grains is formed at the fusion zone border in AZ80 (see white arrows in Figs. 4 and 5).

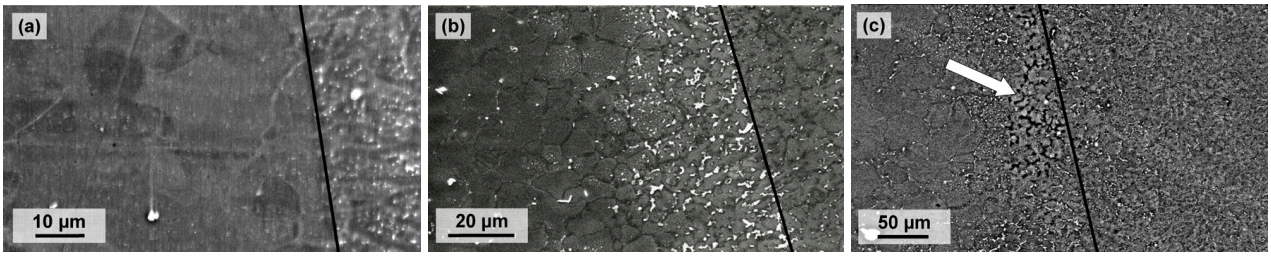

Fig. 4. Cross sectional SEM images of the similar and dissimilar Mg-Al-Zn Mg-alloys: (a) AZ31B-AZ31, (b) AZ31B-AZ61 and (c) AZ31B-AZ80. Solid black lines are showing distinctly fusion lines between fusion zone and HAZ.

A comparison between the welds with AZ31, AZ61 and AZ80 reveal that this layer with fine equiaxed grains decreases in width with decreasing Al content of the Mg-alloy. In AZ31B-AZ31 laser beam welds no evidence of such layer was found and the micro-structure of this region is equivalent to the microstructure shown in the upper (AZ31B sheet) part of the weld in Fig. 5. These fine equiaxed grains presumably are due to an increase in the number of nucleation sites with increasing precipitate volume of the alloy.

EBSD analysis also reveals texture in the fusion zone to be significantly different from sheet texture. The influence of texture formation in the fusion zone on the mechanical properties of the weld is discussed in detail in [8]. A comparison of fusion zone texture in the different similar and dissimilar welds showed that fusion zone texture does not depend on the Al content of the Mg-alloy.

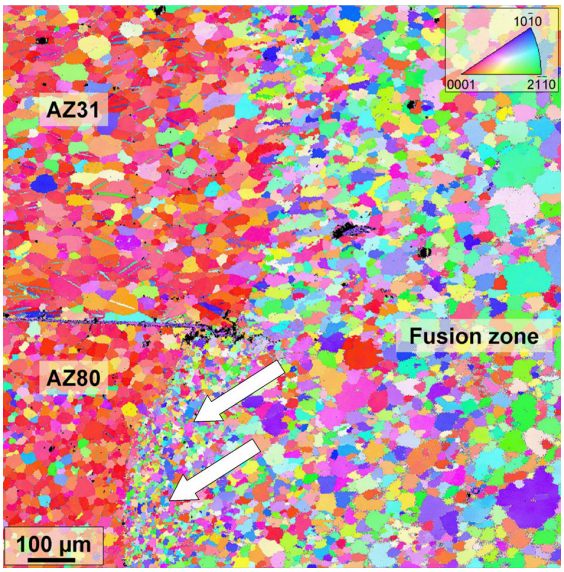

Fig. 5. EBSD inverse pole maps of the interface weld region of the AZ31B-AZ80 configuration.

Mechanical Properties. Microhardness profiles on the cross section of the AZ31B rolled sheets (upper material) are similar in all three welds. The hardness values in the fusion zone (about 57HV0.1) are slightly higher than in the base material (about 53HV0.1). Fig. 6 is showing, as an example, the profiles obtained from AZ31B-AZ80 configuration. Comparing the AZ31, AZ61 and AZ80 profiles an increase in microhardness with increasing Al content of the Mg-alloy is observed [6]. Moreover no pronounced change in hardness is observed from the base material towards to the fusion zone for all configurations. In case of AZ80 a slight increases of hardness is observed in the fine grained zone near the fusion zone border.

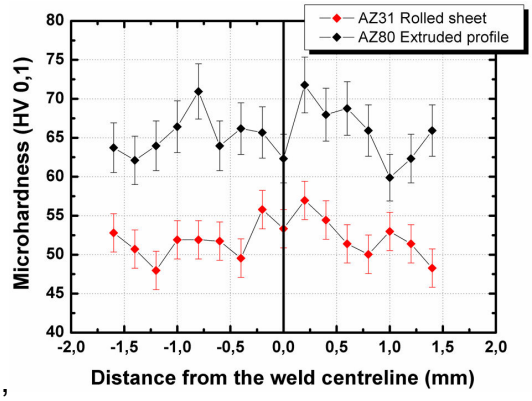

Fig. 6. Micro-hardness profiles of the laser beam welded AZ31B-AZ80 in single overlap configuration.

Residual stresses (RS). The RS distributions obtained for all three locations (Lines 1, 2, 3, see Fig. 2) of the similar AZ31B-AZ31 and dissimilar AZ31B-AZ80 joints are shown in Fig. 7 both in terms of longitudinal and transverse stresses. The RS distributions determined in the AZ31B rolled sheets on top (Line 1, Fig. 2) of the similar (AZ31B-AZ31) and dissimilar (AZ31B-AZ61, AZ31B-AZ80) overlap joints are very similar. This is to be expected due to the welding geometry where in all three welds the AZ31B was on the top. The distribution of longitudinal RS (along the fusion line)

perpendicular to the weld fusion zone is characteristic for fusion welding of materials without phase transformation. The parent material restrains the thermal contraction of the fusion zone in the longitudinal direction, thus, causing tensile stresses within the weld seam and the HAZ. The maximum tensile stress observed in the fusion line reaches 50MPa, which is about one quarter of the typical yield strength (200MPa) of AZ31B [1]. With increasing distance to the seam, the tensile stresses decrease, turning into compressive stresses in the AZ31B base material. The longitudinal RS line profiles are, however, asymmetric with respect to the weld centerline, since the fusion lines are located very close to one of the edges of the Mg-sheet. Low compressive residual stresses are observed with a maximum of -20MPa occurring in the base material (Fig. 7).

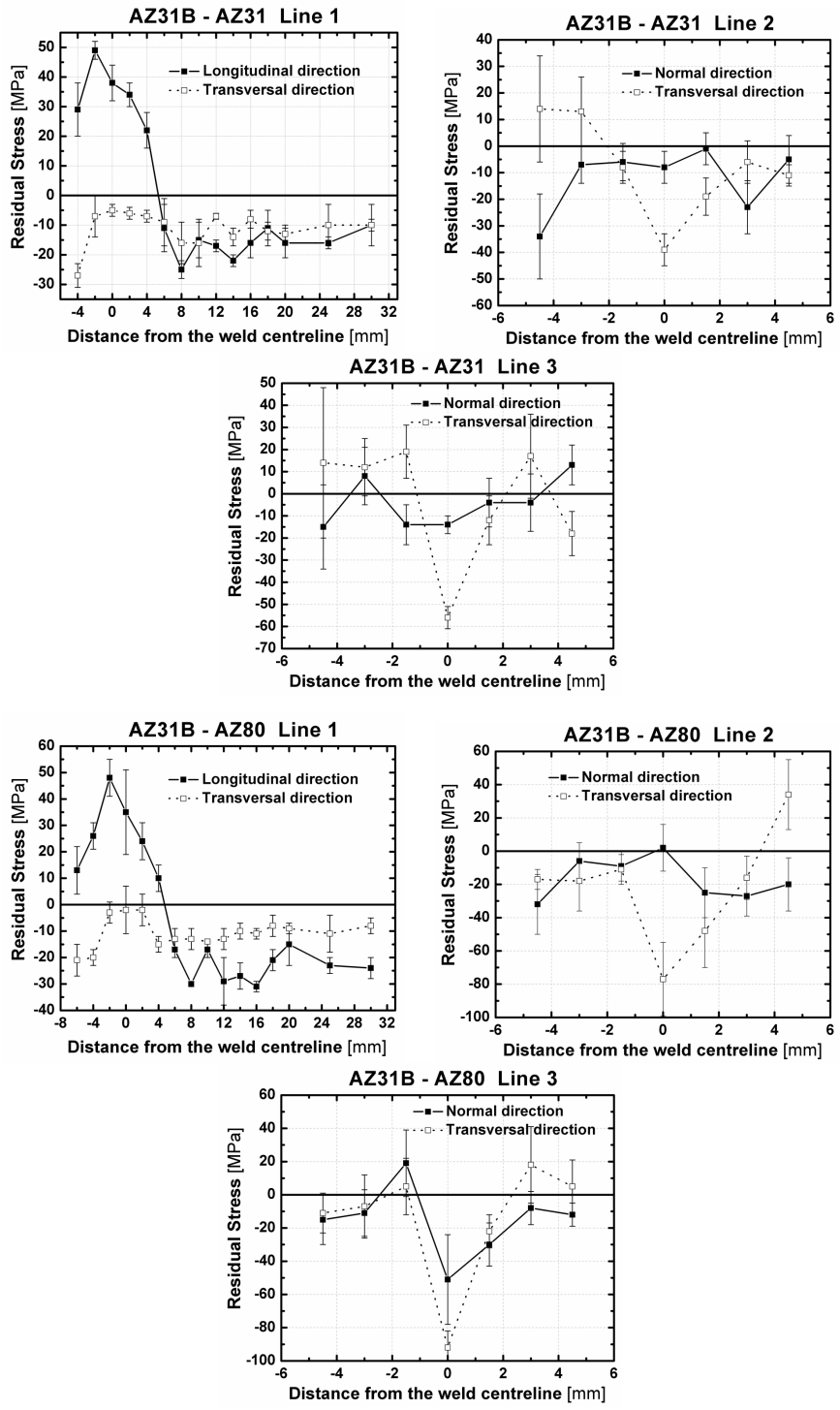

Fig. 7. Residual stress distributions obtained at three different locations (Line 1, 2 and 3, see Fig. 2) in similar and dissimilar overlap joints. On the electropolished cross-sections, compressive residual

stresses are observed at the weld centerline in transversal directions. The base materials tend to be under balancing tensile residual stresses. Comparing the residual stress values obtained in the profiles of the AZ31B-AZ31 and AZ31B-AZ80 (Fig. 7) welds reveals very similar residual stress distributions both in normal and transversal direction. The highest values of compressive stresses are present in the alloy with the higher Al-content AZ80 (see Line 3 in Fig. 7), presumably because the higher Al content is connected with a lower thermal conductivity or higher yield strength especially at high temperature.

Conclusions

Laser beam welds between AZ31B rolled sheets and AZ31, AZ61 and AZ80 extruded L-shape profiles were produced with very good weld qualities. Microstructure analyses reveal that with increasing the Al content of Mg-Al-Zn Mg-alloys the HAZ becomes larger with a network of precipitates ($Mg_{17}(Al,Zn)_{12}$) along the grains boundaries. The RS results show typical profiles characteristic for fusion welding process. Tensile stresses within the fusion zone and the HAZ not larger than one quarter of the typical yield strength of the alloy AZ31B and turns to compressive stresses in the AZ31B base material (Line 1 Fig. 6). The depth analysis on the profiles (Line 3 Fig. 6) shows the highest compressive RS values connected with the highest Al content Mg-alloy.

Acknowledgements

The authors gratefully acknowledge the Helmholtz Association for financial support via the virtual institute ‘Photon and Neutron Research on Advanced Engineering Materials’ (VI-PNAM). HASYLAB at DESY is acknowledge for beam-time at instrument G3 at DORIS. Dr. T. Wroblewski and Dr. A. Rothkirch, HASYLAB, are acknowledged for support during diffraction experiments using synchrotron radiation. R.S.C. thanks the Program Alban - European Union Program of High Level Scholarships for Latin America - for financial support (scholarship No. E04D046587BR).

References

[1] M.M. Avedesian, H. Baker, ASM Specialty Handbook: Mg- and Mg-alloys, ASM International, 1999.
[2] P.G. Sanders, J.S. Keske, K.H. Leong, et al., J. Laser Appl. 11 (2) (1999) 96-103.
[3] K.H. Leong, G. Kornecki, P.G. Sanders, J.S. Keske, ICALEO 98: Laser Materials Processing Conference, Orlando, FL, 16-19 November 1998, pp. 28-36.
[4] X. Cao, M. Jahazi, J.P. Immarigeon et al, J. Mat. Process. Tech. 171 (2006) 188-204.
[5] B.L. Mordike, T. Ebert, Mat. Sci. Eng. A 302 (2001), 37-45.
[6] S. Mueller, K. Mueller, H. Tao, W. Reimers, Int. J. Mat. Res. 97 (2006) 10.
[7] J. Swiostek, J. Bohlen, D. Letzig, K.U. Kainer, in: H.I. Kaplan (Ed.) Mg- Technology (2003) 278.
[8] R.S. Coelho, A. Kostka, H. Pinto, S. Riekehr, M. Koçak, A.R. Pyzalla, Mat. Sci. Eng. A (2007) doi:10.1016/j.msea.2007.07.073.
[9] S.H. Wu, J.C. Huang et al., Metall. Mater. Trans. A, 2004, vol.35A, pp. 2455-2469.
[10] J.A. Esparza, W.C. Davis, E.A. Trillo et al., J. Mat. Sci. Letters, 21 (2002) 917-920.
[11] E. Schubert, M. Klassen, I. Zerner et al., J. Mat. Process. Tech. 115 (2001) 2-8.
[12] M.E. Fitzpatrick, A. Lodini, Taylor & Francis, London, 2003.
[13] C.T Chi, C.G. Chao, T.F. Liu, C.C Wang, Mat. Sci. Eng. A 435-436 (2006) 672-680.
[14] C.T Chi, C.G. Chao, T.F. Liu, C.C Lee, Scripta Materialia 56 (2007) 733-736.